

A combined framework for automated diagnosis and prognosis of structures based on surrogate modelling and a particle filter

Claudio Sbarufatti, Francesco Cadini, Andrea Locatelli and Marco Giglio

Politecnico di Milano, Mechanical Engineering Dept., Milano, 20156, Italy

*claudio.sbarufatti@polimi.it
francesco.cadini@polimi.it
andrea7.locatelli@mail.polimi.it
marco.giglio@polimi.it*

ABSTRACT

Bayesian approaches have proven to be successful in prognostic health monitoring, especially for inverse problem solutions, such as the estimation of damage evolution model parameters from some damage dependent observations. In practice, they stem from the evaluation of the posterior distribution of a vector of parameters of interest conditioned on the observation of some signal features, which relies on the direct calculation of the observation likelihood, i.e. a measure of the probability that the observations are associated to some realizations of the system parameter vector. However, for realistic structures, a numerical simulation might be required for the evaluation of each sample likelihood, which can make the whole procedure for posterior pdf estimation computationally unfeasible.

In this work, this problem is addressed by leveraging on surrogate modelling. Particle filter is used as a general framework for the combined health state estimation and prognosis of a skin panel subject to fatigue crack growth, while observing the strain field pattern acquired at some specific locations. A surrogate model consisting of an artificial neural network, trained on a set of analytical simulations, is used to predict the strain as a function of the crack position and length, thus allowing a fast calculation of the strain observation likelihood. The algorithm is tested with an analytic case study of a crack propagating in an infinite plate, allowing for a simultaneous diagnosis of the crack position and length, as well as a real-time updating of the evolution model parameters and system prognosis.

1. INTRODUCTION

In the last years, scientific and industrial communities have put a lot of efforts into the development of new frameworks for the autonomous assessment of structural integrity,

Claudio Sbarufatti et al. This is an open-access article distributed under the terms of the Creative Commons Attribution 3.0 United States License, which permits unrestricted use, distribution, and reproduction in any medium, provided the original author and source are credited.

generally known as Structural Health Monitoring (SHM), and for the real-time extrapolation of the SHM information into the future, often referred to as Prognostic Health Management (PHM). A combined usage of the two disciplines should allow real-time, automatic evaluations of the state of the structures based on a network of permanently installed sensors, then predicting the future state evolution potentially leading to large operative cost reductions and to the improvement of safety margins.

Many SHM and PHM methods exist in the literature, either based on data (Yuen & Ortiz, 2017, Deraemaeker, Reynders, De Roeck & Kullaa, 2008) or on models (Warner, Bomarito, Hochhalter, W. Leser, P. Leser & Newman, 2017). Data-driven methods often make use of pattern recognition or machine learning approaches for processing actual measurements, in an attempt to diagnose the structural condition and to perform prognosis, without needing to derive any detailed physics-based structural models (Farrar & Worden, 2012, Yan & Wang, 2008, Sbarufatti, Cadini & Giglio, 2017). Conversely, model-based approaches often consider the availability of simulated signal features for the healthy and damaged conditions (Sbarufatti, 2017), that are used to identify the most likely actual state, as well as state evolution models to predict the damage future behaviour (Cadini, Zio & Avram, 2009).

Focussing on model-based SHM and PHM scenarios, they similarly require the solution of inverse problems (Warner et al., 2017) for model updating. For SHM, this implies the identification of damage parameters in a structural model (e.g. fatigue crack position and extension or delamination area for composite materials) based on some features extracted from indirect observations. For PHM, this typically consists in adjusting the evolution model parameters based on a sequence of state observations thus providing a more accurate and precise prognosis. However, this similarity is still overlooked in the literature. A common approach is that of performing damage identification first, and then providing the SHM results as an input to PHM algorithms for damage prognosis and risk assessment, either in a model-based

(Sbarufatti, Corbetta, Manes & Giglio, 2015) or data-driven (Mahadevan, Neal, Nath, Bao, Cai, Orme, Adams & Agarwal, 2017) framework, potentially inducing errors in the resulting statistics.

In this context, Bayesian Model Updating (BMU) techniques offer the opportunity to define a unified statistical framework for damage identification and prognosis, in which the joint posterior probability density function (pdf) of damage and its evolution model parameters are calculated as a function of the observations from indirect measurements. However, it is widely recognised in the literature that a closed form solution of this problem is not available for realistic applications, thus one typically resorts to approximated solutions via Monte-Carlo Sampling (MCS). Among the MCS approaches, Particle Filters (PF), a sequential version of the MCS, have attracted the attention of many researchers in the field of diagnosis and prognosis of structures, due to their demonstrated capability to sequentially update the pdfs of the system parameters in real-time during system observation, within a unique and coherent framework.

However, as for the BMU in general, PF entails the calculation of each sample likelihood for the posterior pdf approximation, which is impractical for real-time diagnostic and prognostic model-based scenarios. In fact, for realistic structures, this would require running a structural model (e.g. based on Finite Element theory) for each sample of the parameter vector. Taking inspiration from the field of structural reliability analysis (Dubourg, 2011, Cadini, Santos & Zio), where similar issues have been successfully addressed in the last decade, surrogate modelling, e.g. based on Artificial Neural Networks (ANN) (Bishop, 2005), can be used to overcome this problem, mapping the inverse relationship between the damage parameters and the numerical signal feature prediction, thus enabling fast likelihood assessment. A noticeable example is reported by Warner et al. (2017), although limited to the diagnosis of damage on the basis of a Markov-Chain Monte Carlo Metropolis-Hastings algorithm. Surrogate models have also been applied to prognostics, specifically leveraging on machine learning for the fast calculation of the stress intensity factor at the crack tip, thus enabling fast damage evolution simulations (Leser, Hochhalter, Warner, Newman, Leser, Wawrzynek & Yuan, 2017, Corbetta, Sbarufatti, Manes & Giglio, 2015).

This study presents a combined stochastic framework for the diagnosis and the prognosis of fatigue damage based on a distributed network of strain field measures. A PF algorithm estimates the joint posterior probability of crack length and crack centre position coordinates, as well as two parameters of a Fatigue Crack Growth (FCG) model, the Paris's law, and the Residual Useful Life (RUL). A surrogate model, consisting of an ANN trained off-line with analytical strain field simulations in presence of different crack damages, is used to map the function between damage parameters and the strain field at sensor location, thus enabling fast sample

likelihood calculation in the PF routine. The algorithm is tested in a simulated framework.

The paper is structured as follow. Section 2 is a review of the PF framework including a discussion on the application of surrogate models for likelihood calculation. The application framework is described in Section 3 and results are shown in Section 4. A conclusive section is finally provided.

2. REVIEW OF PARTICLE FILTER FRAMEWORK

The objective of the filtering problem is to recursively estimate the augmented state of a system, including n_s state variables \mathbf{x} and a vector of n_p parameters $\boldsymbol{\vartheta}$. This system is governed by a dynamic state-space (DSS) model (Haug, 2005) which composes of the evolution equation, $f(\cdot)$, describing the system's dynamics, and the observation equation, $g(\cdot)$, which links the measurements with the true (hidden) system's state. Equation (1) shows the discrete form of the DSS model, which satisfies the first order Markovian assumption (Arulampalam, Maskell, Gordon, & Clapp, 2002).

$$\begin{aligned} \mathbf{y}_k &= f(\mathbf{y}_{k-1}, \mathbf{u}_{k-1}, \boldsymbol{\omega}_{k-1}), \mathbf{y}_k = [\mathbf{x}_k, \boldsymbol{\vartheta}_k] \\ \mathbf{z}_k &= g(\mathbf{y}_k, \boldsymbol{\eta}_k) \end{aligned} \quad (1)$$

The vector $\mathbf{y} \in D \subseteq \mathbb{R}^{n \times 1}$ collects the system's augmented state variables, with $n = n_s + n_p$, $\mathbf{z} = [z_1, z_2, \dots, z_s]^T \in D_z \subseteq \mathbb{R}^{s \times 1}$ is the observation vector, with s the number of sensors, and the subscript k indicates the discrete k -th time step. The state-space domain D is the physical domain of the system's augmented state variables, represented by a partition of the set $\mathbb{R}^{n \times 1}$.

The evolution function depends on the input \mathbf{u} , the model parameters $\boldsymbol{\vartheta}$ and the process noise, $\boldsymbol{\omega}$. A common assumption is that the input of the system \mathbf{u} is observable, and its observability is not further discussed henceforth. The measurement is governed by $g(\cdot)$ and affected by the measurement noise, $\boldsymbol{\eta}$. The noises are random processes transforming the deterministic equations into stochastic equations.

Particle filtering aims at estimating the posterior pdf of \mathbf{y}_k given the sequence of noisy observations $\mathbf{z}_{0:k}$, $p(\mathbf{y}_k | \mathbf{z}_{0:k})$, in case of nonlinear and non-Gaussian systems. The posterior pdf can be approximated by N_s weighted samples (also called particles) of the system's state, as expressed in the Eqs. (2)-(3) (Haug, 2005, Arulampalam et al., 2002, Doucet, Godsill & Andrieu, 2000).

$$\hat{p}(\mathbf{y}_k | \mathbf{z}_{0:k}) = \sum_{i=1}^{N_s} w_k^{(i)} \delta_{\mathbf{y}_k^{(i)}, \mathbf{y}_k} \quad (2)$$

$$\begin{aligned} \bar{w}_k^{(i)} &= w_{k-1}^{(i)} p(\mathbf{z}_k | \mathbf{y}_k^{(i)}) \\ w_k^{(i)} &= \frac{\bar{w}_k^{(i)}}{\sum_{j=1}^{N_s} \bar{w}_k^{(j)}} \end{aligned} \quad (3)$$

where $\hat{p}(\mathbf{y}_k | \mathbf{z}_{0:k})$ is the approximation of $p(\mathbf{y}_k | \mathbf{z}_{0:k})$, $\mathbf{y}_k^{(i)} = [\mathbf{x}_k^{(i)}, \boldsymbol{\theta}_k^{(i)}]$ is the i -th sample of the system's augmented state vector, $w_k^{(i)}$ is the normalized weight of $\mathbf{y}_k^{(i)}$, $p(\mathbf{z}_k | \mathbf{y}_k^{(i)})$ is the likelihood of the observation given $\mathbf{y}_k^{(i)}$ and $\delta_{i, \cdot}$ is the Kronecker delta. The number of samples N_s is supposed to be large enough to describe the (unknown) true shape of $p(\mathbf{y}_k | \mathbf{z}_{0:k})$. It should be noted that Eqs. (2)-(3) refer to the *bootstrap* particle filter (Arulampalam et al., 2002).

The particle filtering-based prognosis is carried out by projecting the samples $\mathbf{x}_k^{(i)}$, $i = 1, \dots, N_s$ many steps ahead in the future, up to a limit state condition, with the p -step ahead prediction equation (Doucet et al., 2000), taking the input \mathbf{u} , the evolution model parameters $\boldsymbol{\theta}$ and the process noise $\boldsymbol{\omega}$, into account. In a scenario for damage evolution prognosis under fatigue load cycles, similarly to (2), the posterior pdf of the number of remaining load cycles $N_{r,k}$ to the critical condition can be estimated at discrete time k as reported in (4) (Cadini et al., 2009):

$$\hat{p}(N_{r,k} | \mathbf{z}_{0:k}) = \sum_{i=1}^{N_s} w_k^{(i)} \delta_{N_{r,k}, N_{r,k}^{(i)}} \quad (4)$$

where $N_{r,k}^{(i)}$ is the number of remaining load cycles to the limit condition, associated to the i -th particle trajectory.

The practical implementation of the algorithm requires the definition of three fundamental functions:

1. The transition density function of the state variables, $p(\mathbf{x}_k | \mathbf{x}_{k-1}, \boldsymbol{\theta}_{k-1})$, which drives the generation of samples $\mathbf{x}_k^{(i)}$ and the p -step ahead prediction equation (Doucet et al., 2000).
2. The transition density function of the parameters, $p(\boldsymbol{\theta}_k | \boldsymbol{\theta}_{k-1})$, which drives the generation of samples $\boldsymbol{\theta}_k^{(i)}$, hereafter based on *Kernel smoothing* approach (Liu & West, 2001).

The likelihood function, $p(\mathbf{z}_k | \mathbf{y}_k^{(i)})$, strictly related to the observation equation (1) and calculated based on the availability of a surrogate model, as discussed in the next paragraph.

2.1. Sample likelihood calculation based on surrogate modelling

In general, likelihood calculation is performed based on the measurement equation (1), by inversely predicting a signal feature for a sample $\mathbf{y}_k^{(i)}$, then calculating an error function between the predicted and the measured features, as in Eq. (5).

$$p(\mathbf{z}_k | \mathbf{y}_k^{(i)}) = \frac{1}{(2\pi\sigma_{\eta,k}^2)^{s/2}} \exp\left(-\frac{1}{2\sigma_{\eta,k}^2} \sum_{j=1}^s (z_k^j - g^j(\mathbf{x}_k^{(i)}, \boldsymbol{\eta}_k))^2\right) \quad (5)$$

where $\sigma_{\eta,k}^2$ is the variance of $\boldsymbol{\eta}_k$. Notice that, without any loss of generality, hereafter the parameter vector $\boldsymbol{\theta}_k$ is not included as input for $g(\cdot)$, assuming the signal feature is only influenced by the state variables in \mathbf{x}_k . This calculation is repeated N_s times at each k -th discrete time. In a model-based framework this means running a model simulation each time a new likelihood assessment is required, which is often impractical if no analytical closed form solution exists for $g(\cdot)$, as this would lead to very high computational effort, preventing a *real-time* application of the method.

It is thus possible to run *off-line* a number of simulations by a high fidelity model for S_M state conditions $\mathbf{x}^{(i)}$, $i = 1, \dots, S_M$, possibly covering most of the state space domain and extracting for each case the simulated versions of the s measured features. This results in a input-output database consisting of a $n_s \times S_M$ input matrix and a $s \times S_M$ output matrix.

The high fidelity model can thus be replaced by a computationally efficient surrogate model for *real-time* operation, mapping the input-output relation intrinsic to the available database. The latter can be accomplished in a machine learning framework, for example, leveraging on regression ANNs, as in the present study. For brevity, it is not the authors intention to enter into the details of ANN formulation, as the literature is full of comprehensive descriptions of SHM application (Farrar & Worden, 2012). Here we limit to specify that, in order to limit the ANN complexity and to favour ANN generalization (Bishop, 1995), s ANN surrogate models \mathcal{M} have been trained, each one predicting the feature measured by a single j -th sensor z_k^j as a function of the input sample $\mathbf{x}_k^{(i)}$, $\mathcal{M}^j(\mathbf{x}_k^{(i)})$, thus calculating the observation likelihood as in (6):

$$p(\mathbf{z}_k | \mathbf{y}_k^{(i)}) = \frac{1}{(2\pi\sigma_{\eta}^2)^{s/2}} \exp\left(-\frac{1}{2\sigma_{\eta}^2} \sum_{j=1}^s (z_k^j - \mathcal{M}^j(\mathbf{x}_k^{(i)}))^2\right) \quad (6)$$

Notice that this formulation considers a constant observation noise and does not take model biases into account, thus $\boldsymbol{\eta}_k = \mathcal{N}(0, \sigma_{\eta}^2)$. However, the latter can be easily included if a test program for model validation is carried out, which is outside the scope of the present activity.

3. METHOD APPLICATION TO FCG DIAGNOSIS AND PROGNOSIS

3.1. The simulated FCG and the simulated strain measurements

The method is applied to the prediction of FCG in an infinite aluminium plate subject to stationary sinusoidal load. The plate is supposed to have infinite dimensions (no effect of the plate boundaries on the simulated strain field) and is equipped with a network of $s = 20$ virtual strain gauges (Figure 1),

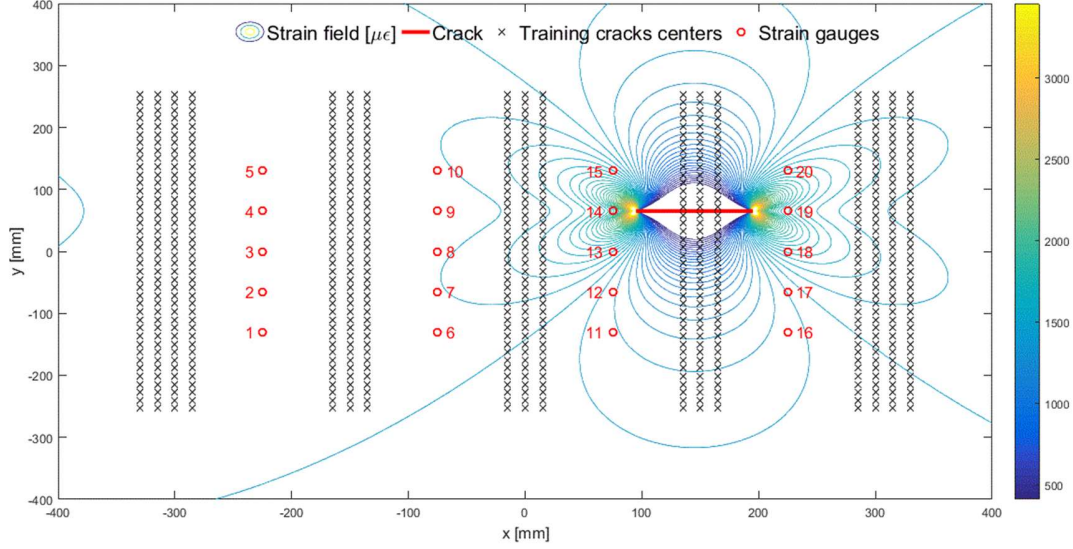


Figure 1. Schematic view of the plate and sensor network positions, with simulated strain field (ε_y) in presence of a crack with centre coordinates [145, 65]mm. The crack centres used for surrogate model training are also indicated.

measuring in y-direction and representative of a network of optical fibre Bragg grating sensors. Sensors layout has been defined based on previous experience by the authors. FCG has been numerically simulated according to Paris's law and based on (7):

$$a_k = a_{k-1} + C (\beta DS \sqrt{\pi a_{k-1}})^m \Delta N \quad (7)$$

a_k indicates the crack length at discrete step k , C and m are two material parameters typical for aluminum, β is the shape function, DS is a known input variable indicating the stress range in one load cycle and ΔN is the load cycle increment for crack step calculation, here set to 100 cycles introducing negligible numerical errors.

The strain measures during simulated FCG are analytically derived. An analytical solution exists for the calculation of the stress field in presence of a crack for very simplified applications (Sanford, 2003). Consider a reference system with origin in the crack centre position, as in Figure 2. The stress solution for the infinite plate in presence of a central crack with length $2a$ and subject to a uniaxial far field stress S (Figure 2.a) is (Sanford, 2003):

$$\begin{aligned} \sigma_x &= \frac{S r}{\sqrt{r_1 r_2}} \cos\left(\theta - \frac{\theta_1 + \theta_2}{2}\right) + \\ &\quad - \frac{S a^2}{(r_1 r_2)^{\frac{3}{2}}} r_1 \sin(\theta_1) \sin\left(\frac{3}{2}(\theta_1 + \theta_2)\right) - S \\ \sigma_y &= \frac{S r}{\sqrt{r_1 r_2}} \cos\left(\theta - \frac{\theta_1 + \theta_2}{2}\right) + \\ &\quad + \frac{S a^2}{(r_1 r_2)^{\frac{3}{2}}} r_1 \sin(\theta_1) \sin\left(\frac{3}{2}(\theta_1 + \theta_2)\right) \end{aligned} \quad (8)$$

$$\tau_{xy} = \frac{S a^2}{(r_1 r_2)^{\frac{3}{2}}} r_1 \sin(\theta_1) \sin\left(\frac{3}{2}(\theta_1 + \theta_2)\right)$$

It allows the calculation of $\sigma_x(x, y)$ and $\sigma_y(x, y)$ stress tensor components, with $x = r \cos(\theta)$ and $y = r \sin(\theta)$ coordinates indicating the relative distance of a sensor from the crack centre. The strain measure in y-direction is thus analytically simulated by applying the constitutive law and adding a Gaussian noise $\eta \sim \mathcal{N}(0, \sigma_\eta^2)$:

$$\varepsilon_y = \frac{\sigma_y(x, y)}{E} - \frac{\nu}{E} \sigma_x(x, y) + \eta \quad (9)$$

where E and ν are the elastic modulus and the Poisson's ratio, respectively. A strain field example is reported in Figure 1, for a 100 mm long crack and with no noise perturbation. The data for the generation of virtual strain observations are summarized in Table 1.

Table 1. Data for generation of target FCG and virtual strain observations.

| Parameter | Value |
|-----------------|--|
| C | $2.382 \cdot 10^{-12}$ [mm/cycle (MPa√mm) ^{-m}] |
| m | 3.2 [-] |
| β | 1 [-] |
| DS | 100 [MPa] |
| a_0 | 5 [mm] |
| σ_η^2 | 25 [με ²] |
| E | 71000 [MPa] |
| ν | 0.3 [-] |

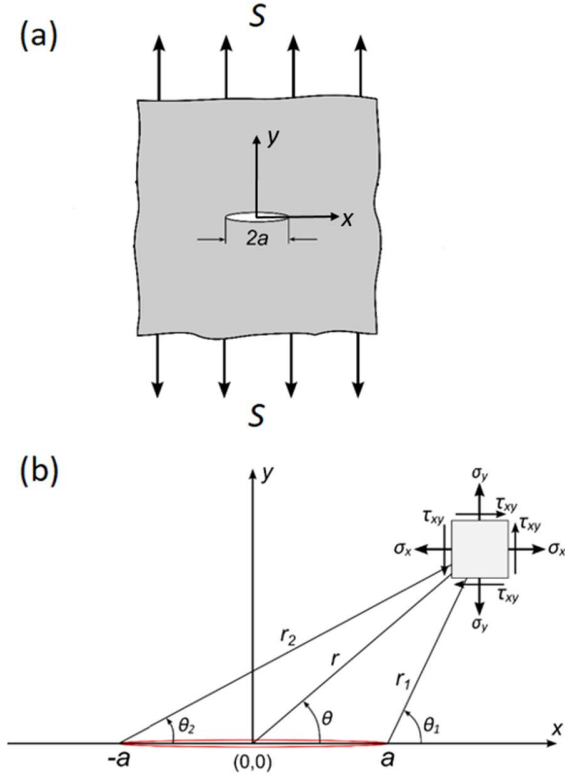


Figure 2. (a) Schematic view of the infinite plate model and (b) reference system for the application of equation (8).

3.2. Particle Filter implementation

In this study, the PF algorithm is configured as a sequential importance resampling algorithm with systematic resampling (Arulampalam et al., 2002) and is used as a unified statistical framework for real-time diagnosis and prognosis of FCG. Diagnosis is performed by filtration of the $n_s = 3$ state variables, which are collected in \mathbf{x} , including crack length a and the x, y coordinates of the crack centre. For crack length, this requires definition of the transition density function of a , $p(a_k | a_{k-1}, \boldsymbol{\vartheta}_{k-1})$, which is obtained by adding a random perturbation, the process noise $\boldsymbol{\omega}$, to Equation (7). The process noise is a representation of non-modelled phenomena and variabilities of true dynamic processes that are not accounted for in typical engineering models. As detailed by some of the authors in (Corbetta, Sbarufatti, Giglio & Todd, 2018), this random perturbation should not significantly modify the trend of the particle swarm, the latter being the goal of the model parameter updating procedure discussed below, while it should enlarge or shrink the particle dispersion. A log-Normal perturbation is selected $\boldsymbol{\omega} \sim \mathcal{N}\left(-\frac{\sigma_\omega^2}{2}, \sigma_\omega^2\right)$ (Corbetta et al., 2018) and, considering $\omega^{(i)}$ is a realization of $\boldsymbol{\omega}$, equation (7) is modified for the i -th particle as:

$$a_k^{(i)} = a_{k-1}^{(i)} + C \left(\beta DS \sqrt{\pi a_{k-1}^{(i)}} \right)^m \Delta N \exp(\omega^{(i)}) \quad (10)$$

For the x, y coordinates, leveraging on the assumption of infinite plate dimensions, it is reasonable to consider a symmetric FCG at the two crack tips, thus a fixed crack centre during damage evolution. A *kernel smoothing* sub-algorithm has thus been used to project samples of the x, y coordinates during run-time. For the i -th particle, samples are drawn according to equation (11), considering x and y coordinates uncorrelated, thus substituting either x or y to the general variable c :

$$c_k^{(i)} = \sqrt{1 - h^2} c_{k-1}^{(i)} + (1 - \sqrt{1 - h^2}) E[c]_{k-1} + r \quad (11)$$

$$c = x, y$$

Where r is a realization of $\mathcal{N}(0, h^2 V[c]_{k-1})$, $h \in [0; 1]$ is the smoothing parameter, a choice of the algorithm designer (Liu & West, 2001), and the two moments $E[c]_{k-1}$ and $V[c]_{k-1}$ are the Monte Carlo-mean and -variance of the centre coordinates at the previous time step, respectively. Specifically, during algorithm initialization, a variance is selected in order to provide x, y samples covering the entire sensor area.

Prognosis is performed by propagating particles many steps ahead in the future, up to a critical crack length, a_{cr} , based on Eq. (10). The latter contains $n_p = 2$ model parameters, collected in the model parameter vector $\boldsymbol{\vartheta} = [C, m]$, which are typically available in the literature for many materials, although affected by very large dispersion (Virkler, 1979, Annis, 2005). Real-time model parameter updating is used to shrink this uncertainty conditional on the observed data, thus aiming at improving the prediction of future trends. Inside the PF framework, this requires sampling of $\boldsymbol{\vartheta}_k^{(i)}$, which is performed, again, based on the *kernel smoothing* sub-algorithm, and taking the statistical correlation of C and m into account (Annis, 2004):

$$\boldsymbol{\vartheta}_k^{(i)} = \sqrt{1 - h^2} \boldsymbol{\vartheta}_{k-1}^{(i)} + (1 - \sqrt{1 - h^2}) E[\boldsymbol{\vartheta}]_{k-1} + \mathbf{r} \quad (12)$$

Where \mathbf{r} is a realization vector of $\mathcal{N}(0, h^2 \Sigma[\boldsymbol{\vartheta}]_{k-1})$ and $\Sigma[\boldsymbol{\vartheta}]_{k-1}$ the Monte Carlo covariance matrix of $\boldsymbol{\vartheta}$ at the previous time step, thus allowing to sample C and m from their joint posterior distribution. The initialization of the model parameters follows the historical data of the Al2024-T3 aluminum alloy found by Virkler, Hillberry and Goel (1979). Table 2 collects the PF hyperparameters and the initialization moments herein adopted.

3.3. The surrogate model for strain prediction

As anticipated in section 3.1, an analytical expression exists for calculation of stresses and strains at j -th sensor position in an infinite plate subject to FCG. For more complex situations, one can make use of numerical simulations, e.g. by means of Finite Elements, for strain prediction at sensor locations, then using a surrogate model to predict the strain at some target

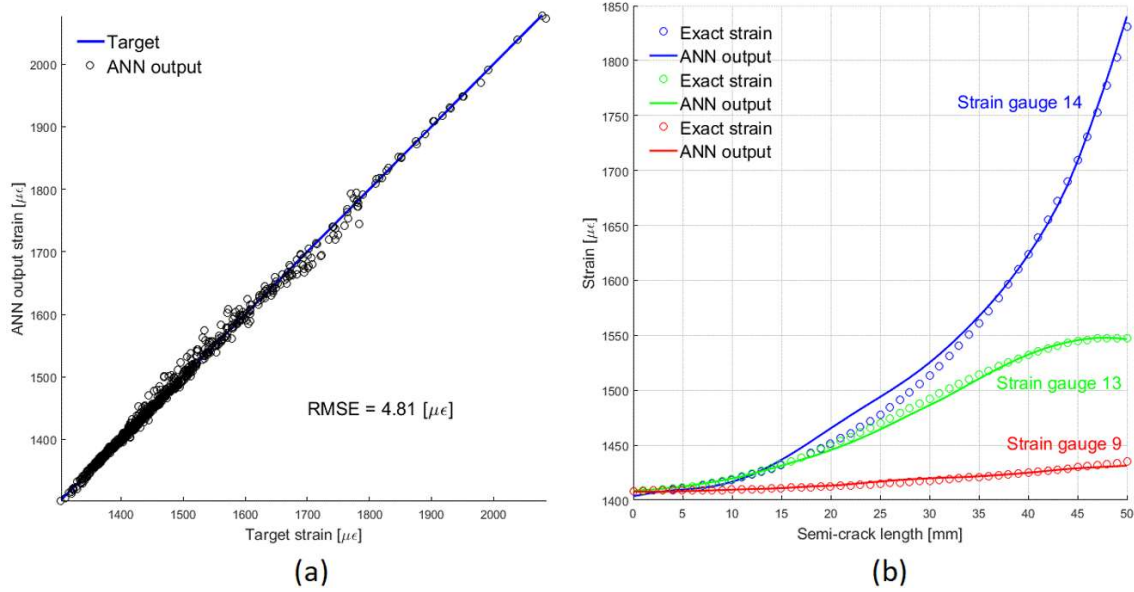


Figure 3. (a) regression plot for ANN performance assessment under a test dataset, (b) strain sensitivity for sensors ID 9, 13 and 14 to a crack propagating in the plate centre.

Table 2. Hyperparameters and initialization variables of the PF framework.

| Parameter | Value |
|---------------------------------|--|
| σ_ω^2 | 1 |
| h | 0.2 |
| $E[c]_0$ | [0,0] mm |
| $V[c]_0$ | [20000,20000] mm ² |
| $E[\boldsymbol{\theta}]_0$ | [2.382 10 ⁻¹² , 3.2] |
| $\Sigma[\boldsymbol{\theta}]_0$ | $\begin{bmatrix} 0.9966 & -0.1764 \\ -0.1764 & 0.0346 \end{bmatrix}$ |
| a_{cr} | 50 mm |

locations for each state particle $\mathbf{x}_k^{(i)}$ representing damage condition, thus allowing calculation of the observation likelihood in (6). For this reason, the complete model-based scenario including the surrogate model is tested hereafter, although the latter could be potentially substituted by the analytical expression in (9) for this rather simplified application.

Twenty Multi-Layer Perceptron ANNs are trained with input-output examples generated with (9), each of them predicting the strain for one j -th sensor included in the network (Figure 1). The j -th ANN is constituted by a 3-node input layer (for $\mathbf{x} = [\mathbf{a}, \mathbf{x}, \mathbf{y}]$), a 1-node output layer (for $\boldsymbol{\epsilon}_y^j$), and a 100-node hidden layer, selected with a trial and error

procedure to guarantee sufficient ANN generalization. The interested reader can refer to Sbarufatti (2017), where the description of a rigorous method for hidden node number selection is provided in the context of model-based damage identification on realistic structures. *Quasi-Newton* optimization algorithm, available in NETLAB (Nabney, 2004), has been selected for ANN training, coupled with *cross validation* and *early stopping* to avoid data overfitting (Bishop, 1995), specifically dividing the training and validation subsets with a 70% - 30% proportion and stopping the training algorithm when the validation error increases for 8 consecutive training epochs. The training database includes 1112 crack centre positions (located as in Figure 1¹) and a variable number of crack lengths depending on the relative distance between the sensor and the crack centre, for a total $S_{\mathcal{M}} = 91376$.

The performance of the surrogate model for strain prediction at sensor ID 7 can be appreciated in Figure 3.a, where the regression plot between target and predicted strains is shown for a new dataset never seen during training and including cracks with different lengths and randomly dispersed over the plate area within the sensor grid. The corresponding root mean square error is 4.81 μϵ. The strain sensitivity of sensors ID 9, 13 and 14 to a crack propagating as in Figure 1 is also shown in Figure 3.b for comparison with the error found for strain field prediction by the ANN. Both the exact target strain (used for training) and the ANN output regression are shown in the same figure.

¹ Training crack centre positions have been selected avoiding any crack crossing the vertical axis intersecting sensor locations, in order to facilitate ANN training.

4. RESULTS

The algorithm performance is now assessed on a simulated FCG, initiated as in Figure 1, based on sequential strain field observations calculated with (9). The target of the test is the estimation of the crack centre coordinates (145mm and 65mm for x and y , respectively) and the crack length, then refining the prior pdf of the evolution model parameters (C and m), finally providing a refined prediction of the RUL. The PF output results have been illustrated in Figures 4-6. The posterior state estimation is shown in 4.a, 4.b and 4.c, for the x,y crack centre coordinates and the crack length, respectively. The RUL posterior pdf is reported in Figure 4.d, calculated with equation (4). In particular, results are shown in terms of mean value and 95% confidence boundaries of the posterior state estimate. Due to the statistical correlation of C and m parameters (Annis, 2004), their joint posterior estimate is represented in Figure 5, in terms of particle dispersions, at three instants of the FCG, specifically at the initiation of the filter, at mid-life and at the end-of-life. Finally, Figure 6

shows the particle projection at future time steps, again for three discrete time instants during FCG.

Up to approximately 5×10^3 cycles, the sequential filter is unable to refine the posterior estimation of the state and parameter variables due to the fact that the observation noise hides the insufficient strain sensitivity to damage. In particular, this is reflected in the large uncertainty affecting the crack centre coordinates, which is coupled with a relatively wrong estimate of the crack length. Then, considering also the large prior uncertainty on C and m parameters (visible in Figure 5 at algorithm initiation, $N=1$), a very low accuracy and precision is found for the RUL prediction. In fact, their prior dispersion, coupled with the uncertainty on the crack length estimation, is responsible for the very wide particle dispersion when projected at future time steps, as visible in Figure 6.a. However, when a significant trend is identified within the observations, after 5×10^3 cycles, the PF algorithm is able to provide very efficient filtering of the state variables, which is reflected in the

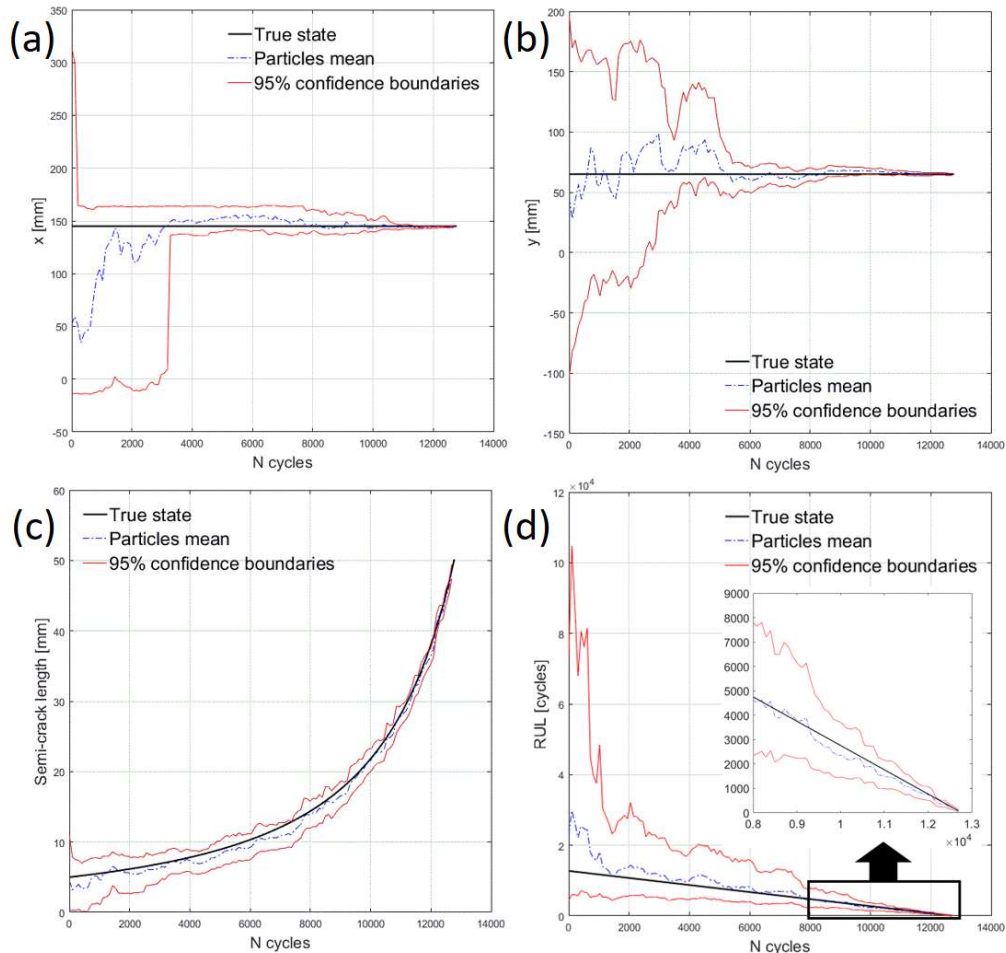


Figure 4. PF results (a) x-coordinate of crack centre, (b) y-coordinate of crack centre, (c) crack length and (d) RUL estimate.

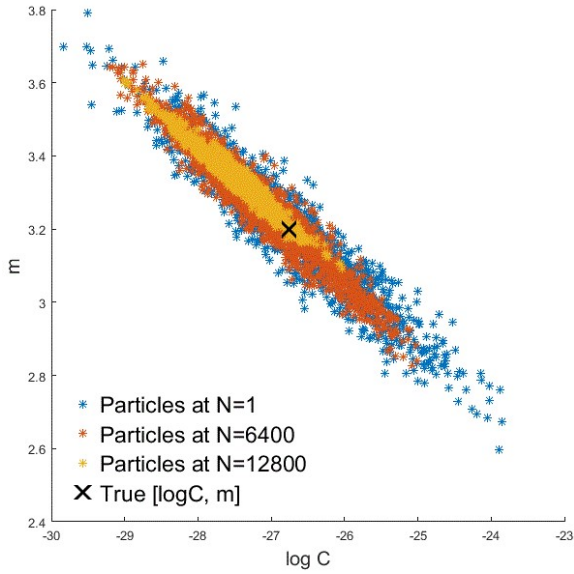


Figure 5. Posterior joint distribution of C and m parameters at three instants during FCG. The true parameters used for target FCG are also displayed.

convergence of the x,y crack centre coordinates and the crack length on the target value, with narrower confidence boundaries, thus resulting in a visible shrinkage of the RUL distribution. The increase of precision in the RUL estimate is also the result of the algorithm ability of filtering the multivariate joint distribution of C and m parameters while the observation trend becomes clearer, diminishing the particle dispersion (Figure 5). The latter is in fact reflected in less particle dispersion when projected at future time steps, as visible in Figure 6.b-c.

5. CONCLUSION

A Particle Filter algorithm is used in this study as a unique statistical framework for diagnosis and prognosis of structures subject to fatigue crack growth, providing real-time estimation of the damage parameters, including crack centre coordinates and crack length, updating of two fatigue crack model parameters, and prediction of residual life distribution, conditioned on sequential strain observations. The algorithm is tested in a rather simplified scenario consisting of a crack propagation in an infinite plate subject to a far field stress, for which the exact analytical strain field solution exists and is used to generate strain observations during FCG, upon addition of random Gaussian noise to simulate a realistic measurement.

One limit to the real-time implementation of the method is the requirement for very fast likelihood assessment, for each Monte-Carlo sample at each observation. Though this obstacle could be easily overcome in this simplified scenario due to the availability of an analytical function predicting the strain at sensor positions as a function of the damage

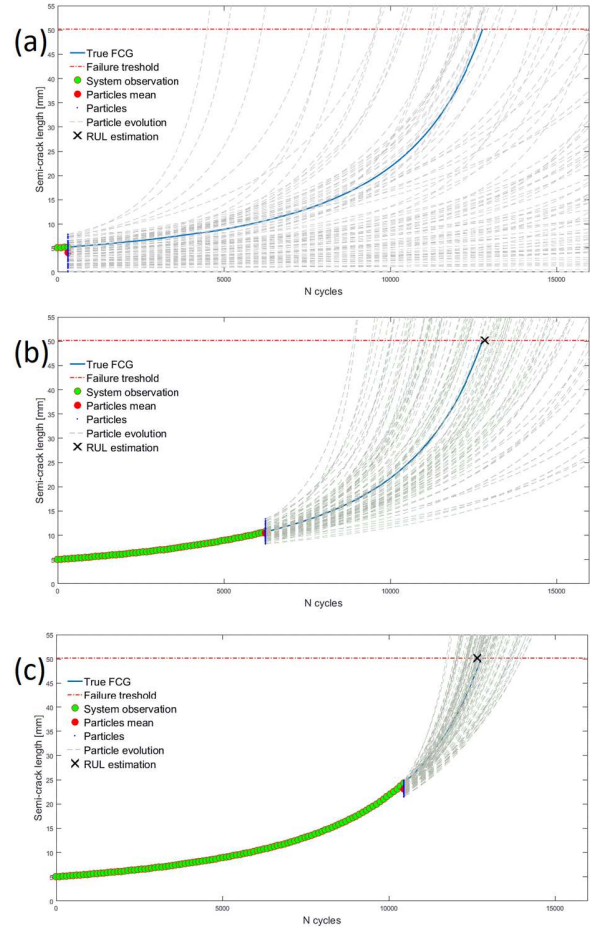


Figure 6. Particle projection for RUL pdf estimation at three instants during FCG.

characteristics, i.e. the crack length and the crack centre coordinates, a more general approach is used, which is valid also when no analytical strain field solutions exist. In practice, a surrogate model consisting of an artificial neural network is trained off-line with a database of analytical strain patterns for different damage examples. During the algorithm on-line operation, the ANN takes a state sample as input (including the sampled crack length and crack centre coordinates) and provides the strain at sensor locations as output, for instantaneous sample likelihood calculation. The results shown in this paper are very optimistic and the algorithm real-time effectiveness for contemporaneous tracking of the damage variable, for diagnosis, and updating of the damage evolution model parameters, for prognosis, has been proven. Thus, the method extension for more complex monitoring scenarios, based on a database of numerical strain patterns for various damage examples, is matter of the future extension by the authors.

Nevertheless, as most of the Monte-Carlo sampling methods in the literature, the method suffers for sampling impoverishment in case of a wrong selection of its hyper-

parameters, including the process noise and the parameter sampling variances. In this study, this selection is facilitated by using an optimal unbiased process noise and the *kernel smoothing* sub-algorithm for parameter sampling. However, future research should target the identification of quantitative probabilistic methods to select these fundamental particle filtering parameters.

NOMENCLATURE

| | |
|--------------------------------|--|
| a | semi-crack length |
| a_0 | initial semi-crack length for propagation initialization |
| a_{cr} | critical semi-crack length for residual life calculation |
| C | material parameter in Paris's law |
| DS | stress range in one load cycle |
| E | Young's modulus |
| $f(\cdot)$ | evolution equation |
| $g(\cdot)$ | observation equation |
| h | Kernel smoothing parameter |
| k | discrete time step |
| m | material parameter in Paris's law |
| \mathcal{M}^j | surrogate model for feature prediction at j -th sensor |
| n | number of elements in \mathbf{y} |
| n_p | number of parameters in $\boldsymbol{\vartheta}$ |
| n_s | number of state variables in \mathbf{x} |
| N_s | number of particles |
| N_r | number of remaining load cycles to critical condition |
| r, \mathbf{r} | perturbation sample (or sample vector) for parameter updating |
| $r_1, r_2, \theta_1, \theta_2$ | geometrical parameters for stress calculation |
| s | number of sensors |
| $S_{\mathcal{M}}$ | number of example states for surrogate model training |
| S | far field stress |
| \mathbf{u} | input parameters of the evolution model |
| $w_k^{(i)}$ | normalised weight of the i -th particle |
| $\bar{w}_k^{(i)}$ | non-normalised weight of the i -th particle |
| x, y | crack centre coordinates |
| \mathbf{x} | vector of state variables |
| \mathbf{y} | augmented state vector $\mathbf{y} = [\mathbf{x}, \boldsymbol{\vartheta}]$ |
| $\mathbf{y}_k^{(i)}$ | i -th sample of \mathbf{y} at k -th discrete time |
| $\mathbf{x}_k^{(i)}$ | i -th sample of \mathbf{x} at k -th discrete time |
| \mathbf{z} | observation vector |
| β | shape function |
| δ_{\cdot} | Kronecker delta |
| ε_y^j | strain observation in y -direction by the j -th sensor |
| ΔN | load cycle increment for numerical crack propagation |
| σ_{η}^2 | variance of $\boldsymbol{\eta}$ |
| σ_{ω}^2 | variance of process noise $\boldsymbol{\omega}$ |
| σ_x, σ_y | stress tensor components in x, y -direction |

| | |
|--------------------------|---|
| ν | Poisson's ratio |
| $\boldsymbol{\vartheta}$ | vector of parameters for model updating |
| $\boldsymbol{\omega}$ | process noise |
| $\boldsymbol{\eta}$ | measurement noise |

REFERENCES

- Annis, C. (2004). Probabilistic life prediction isn't as easy as it looks. *ASTM Special Technical Publication*, (1450), pp. 3-14.
- Arulampalam, M. S., Maskell, S., Gordon, N., & Clapp, T. (2002). A tutorial on particle filters for online nonlinear/non-gaussian bayesian tracking. *Signal Processing, IEEE Transactions on*, 50(2), pp. 174–188.
- Bishop, C. M. *Neural Networks for Pattern Recognition*. Ed. Oxford University Press, 1995.
- Cadini, F., Zio, E., Avram, D. (2009). Monte Carlo-based filtering for fatigue crack growth estimation. *Probabilistic Engineering Mechanics*, 24 (3), pp. 367-373.
- Cadini, F., Santos, F., Zio, E. (2014). An improved adaptive kriging-based importance technique for sampling multiple failure regions of low probability. *Reliability Engineering & System Safety*, Vol. 131, pp. 109-117.
- Corbetta, M., Sbarufatti, C., Giglio, M., Todd, M.D. (2018). Optimization of nonlinear, non-Gaussian Bayesian filtering for diagnosis and prognosis of monotonic degradation processes. *Mechanical Systems and Signal Processing*, 104, pp. 305-322.
- Deraemaeker, A., Reynders, E., De Roeck, G., & Kullaa, J. (2008). Vibration-based structural health monitoring using output-only measurements under changing environment. *Mech. Syst. Signal Process*, vol. 22, no. 1, pp. 34–56.
- Doucet, A., Godsill, S., & Andrieu, C. (2000). On sequential monte carlo sampling methods for bayesian filtering. *Statistics and computing*, 10(3), pp. 197–208.
- Dubourg, V. (2011). *Adaptive surrogate models for reliability analysis and reliability-based design optimization*. Doctoral Dissertation. Université Blaise Pascal - Clermont-Ferrand II.
- Farrar, C. R., & Worden, K. (2012). *Structural health monitoring: a machine learning perspective*. John Wiley & Sons.
- Haug, A. (2005). A tutorial on bayesian estimation and tracking techniques applicable to nonlinear and non-gaussian processes. *MITRE Corporation, McLean*.
- Leser, P.E., Hochhalter, J.D., Warner, J.E., Newman, J.A., Leser, W.P., Wawrzynek, P.A., Yuan, F.-G. (2017). Probabilistic fatigue damage prognosis using surrogate models trained via three-dimensional finite element analysis, *Structural Health Monitoring*, 16 (3), pp. 291-308.
- Liu, J., & West, M. (2001). Combined parameter and state estimation in simulation-based filtering. *In Sequential monte carlo methods in practice*, pp. 197–223, Springer.

- Mahadevan, S., Neal, K., Nath, P., Bao, Y., Cai, G., Orme, P., Adams, D., Agarwal, V. (2017). Quantitative diagnosis and prognosis framework for concrete degradation due to alkali-silica reaction. *AIP Conference Proceedings*, 1806, art. no. 080006.
- Nabney, I. T. (2004). *NETLAB Algorithms for pattern recognition*, Springer - Verlag, London.
- Sanford, R. J. (2003). *Principles of fracture mechanics*, ISBN: 978-0130929921.
- Sbarufatti, C., Cadini, F., Giglio, M. (2017). Adaptive prognosis of fatigue damage based on the combination of particle filters and neural networks. *Proceedings of the 11th International Workshop on Structural Health Monitoring, IWSHM 2017*, 1, pp. 623-630.
- Sbarufatti, C. (2017). Optimization of an artificial neural network for fatigue damage identification using analysis of variance. *Structural Control and Health Monitoring*, 24 (9), art. no. e1964.
- Sbarufatti, C., Corbetta, M., Manes, A., Giglio, M. (2015). Sequential Monte-Carlo sampling based on a committee of artificial neural networks for posterior state estimation and residual lifetime prediction. *International Journal of Fatigue*, 83, pp. 10-23.
- Corbetta, M., Sbarufatti, C., Manes, A., Giglio, M. (2015), Real-time prognosis of crack growth evolution using sequential Monte Carlo methods and statistical model parameters, *IEEE Transactions on Reliability*, 64 (2), art. no. 6953312, pp. 736-753.
- Virkler, D., Hillberry, B., Goel, P. (1979). The statistical nature of fatigue crack propagation, *Journal of Engineering Materials and Technology*, 101 (2), pp. 148-153.
- Warner, J. E., Bomarito, G. F., Hochhalter, J. D., Leser, W. P., Leser, P.E., & Newman, J.A. (2017). A Computationally-Efficient Probabilistic Approach to Model-Based Damage Diagnosis. *Int. J. Progn. Heal. Manag.*, vol. 8.
- Yan, J. H., Wang, P. X. (2008). Prognosis of blade material fatigue using Elman Neural Networks. *Applied Mechanics and Materials*, 10-12, pp. 558-562.
- Yuen, K. V., & Ortiz, G. A. (2017). Outlier detection and robust regression for correlated data, *Comput. Methods Appl. Mech. Eng.*, vol. 313, pp. 632-646.

BIOGRAPHIES

Claudio Sbarufatti is a research scientist and Assistant Professor with the Department of Mechanical Engineering at Politecnico di Milano, Italy. His research interests include

model-based diagnosis and prognosis of mechanical and aerospace components, Monte-Carlo methods for Bayesian model updating and filtering, inverse problems for load monitoring, distributed sensing, system failure modeling, impact modeling on composite structures. He is currently involved in the management of international projects mainly focused on structural health monitoring, load monitoring and residual life prognosis.

Francesco Cadini is assistant professor at the Department of Mechanical Engineering of the Politecnico di Milano. His main research efforts are currently devoted to the quantitative treatment of uncertainties affecting the models for risk assessment and mitigation in modern engineering systems. In particular, his activities are mainly focused on the development and application of i) sequential Monte Carlo algorithms (particle filters) for state estimation and prediction with applications to system diagnostic and prognostic, ii) variance reduction methods for more efficient Monte Carlo-based uncertainty analysis, iii) surrogate modeling (neural networks, polynomial chaos expansion, kriging, fuzzy logic, support vector machine, etc.) for model identification, time series prediction and optimal control in complex engineering systems.

Andrea Locatelli obtained the Bachelor in Mechanical Engineering in 2016 at Politecnico di Milano, where he is going to succeed in the Master of Science in Mechanical Engineering, specialising in "Advanced Mechanical Design". His current work of master thesis is focused on Structural Health Monitoring, aimed at the diagnosis and residual life prognosis of mechanical components, in a probabilistic framework. The methodologies of interest are based on particle filter strategy, combined with surrogate models generated by artificial neural networks.

Marco Giglio is Full Professor of Mechanical Design and Strength of Materials, and works in the Department of Mechanical Engineering at Politecnico di Milano, Italy. His research fields are novel methods for SHM application, ballistic damage and evaluation of the residual strength, methods of fatigue strength assessment in mechanical components subjects to multiaxial state of stress, design and analysis of helicopter components with defects, optimization of structures for energy application. He is the author of over 150 scientific papers in international journals and conferences and is a member of scientific associations (AIAS, Italian Association for the Stress Analysis, IGF, Italian Group Fracture).